Particle-size distributions from Fraunhofer diffraction: the singular-value spectrum

1985 Inverse Problems 1 111

(http://iopscience.iop.org/0266-5611/1/2/003)

Inverse Problems 1 (1985) 111–126. Printed in Great Britain

Particle-size distributions from Fraunhofer diffraction: the singular-value spectrum

M Bertero†, P Boccacci‡ and E R Pike§

† Istituto Matematico dell'Universitá and Istituto Nazionale di Fisica Nucleare, Genova, Italy

‡ Istituto di Mineralogia dell'Universitá, Genova, Italy

§ Royal Signals and Radar Establishment, St Andrews Road, Great Malvern, Worcs WR14 3PS, UK

Received 8 October 1984, in final form 10 December 1984

Abstract. The results of a previous paper, in which resolution limits were calculated for particle-size distributions determined from Fraunhofer diffraction data, are extended to cover the case of finite sampled data by the use of singular-system techniques, both in weighted and unweighted L^2 spaces. The new results show that knowledge of finite support of the distribution can more than compensate the loss of experimental knowledge of diffraction data due to sampling and truncation.

1. *Introduction*

In a previous paper [1], hereafter referred to as I, the problem of the determination of a particle-size distribution by means of its Fraunhofer diffraction pattern was considered. Eigenfunction expansions were used in order to solve the first-kind Fredholm integral equation

$$g(s)=\int_0^{+\infty} K(st)f(t)\,\mathrm{d}t \tag{1.1}$$

where

$$K(x)=J_1^2(x)/x^2 \tag{1.2}$$

and

$$t=ka=2\pi a/\lambda \qquad f(t)=t^4p(t). \tag{1.3}$$

Here λ is the wavelength of the incident beam, $p(a)\delta a$ is the probability that a particle has a radius in the range a to $a+\delta a$ and $g(s)$ is the intensity scattered at angle s.

In I the solution of equation (1.1) was investigated by assuming that the 'diffraction pattern' $g(s)$ is given for any value of s. This assumption permits an analytical treatment of the problem of the determination of the resolution limits in particle size which can be achieved by means of Fraunhofer diffraction. As explained in I, however, this approach is unphysical for the following reasons.

First of all, equation (1.1) holds true only in the case of small angles, normally $s\sim\sin s$; secondly the form used for the diffraction pattern of an opaque particle is valid only when

0266-5611/85/020111+16 $02.25

the radius a of the particle is much greater than the wavelength λ, say $a > 10\lambda$. Therefore we must replace equation (1.1) by

$$g(s) = \int_{t_0}^{t_1} K(st) f(t)\, dt \qquad s_0 \leqslant s \leqslant s_1 \tag{1.4}$$

where s_0 and s_1 are, respectively, a lower and an upper bound for the diffraction angle (with $s_1 \ll 1$) and t_0 and t_1 are, respectively, a lower and an upper bound for the radius of the particles (with $t_0 \gg 2\pi$, i.e. $a \gg \lambda$).

Equation (1.1) is based on scalar diffraction theory and even with $a > 10\lambda$ it will fail in real experimental situations where the difference in refractive index between the particles and the suspension medium is too small. In more recent commercial equipment using this technique a modification in which K is given by the anomalous scattering formula has been introduced to cover this case. We shall consider this situation in a further paper, but here we concentrate entirely on the Fraunhofer scattering limit.

We assume that $f(t)$ is square integrable (which is equivalent to assuming that $t^4 p(t)$ is square integrable) and we introduce the new variables

$$x = t_0 s \qquad y = t/t_0 \tag{1.5}$$

and also the parameters

$$\gamma = t_1/t_0 \qquad x_0 = t_0 s_0 \qquad x_1 = t_0 s_1. \tag{1.6}$$

Furthermore, if we define the new functions

$$\psi(x) = \frac{1}{\sqrt{t_0}}\, g\left(\frac{x}{t_0}\right) \qquad \varphi(y) = \sqrt{t_0}\, f(t_0 y) \tag{1.7}$$

(the choice of the multiplicative constants preserves normalisation, with respect to the L^2 norm, both of the unknown function and of the data), then equation (1.4) takes the form

$$\psi(x) = \int_1^{\gamma} K(xy)\varphi(y)\, dy \qquad x_0 \leqslant x \leqslant x_1. \tag{1.8}$$

An estimate of the order of magnitude of the parameters involved in equation (1.8) is given by the following remark: if we take the lower radius $a_0 = 10\lambda$ and x_1 corresponding to the second zero of $J_1(x)/x$, namely $x_1 = 7.016$, then we have $s_1 = x_1/t_0 = \lambda x_1/2\pi a_0 = 0.1117$ and $s_1 \simeq \sin s_1$ with an error of the order of 0.2%.

The operator K defined by

$$(K\varphi)(x) = \int_1^{\gamma} K(xy)\varphi(y)\, dy \qquad x_0 \leqslant x \leqslant x_1 \tag{1.9}$$

is a linear compact operator from $L^2(1, \gamma)$ into $L^2(x_0, x_1)$ and therefore singular function expansions, which have been already used by the authors both in Laplace transform inversion [2–4] and in inverse problems related to microscopy [5–8], can be applied to the solution of equation (1.8).

However, from the numerical computations of the singular system of the operator (1.9) (reported in §5) it follows that the singular functions in the solution space have a troublesome behaviour at the edges of the interval $[1, \gamma]$; in fact, they are very large there and therefore they are large precisely in those regions where the unknown solution is presumably small. This behaviour, which has been found by the authors also in the case of

Laplace transform inversion [4, 9], gives rise to spurious edge effects which deteriorate the restored solution [9].

A route for overcoming this difficulty is to look for solutions in weighted L^2 spaces, i.e. to require that the unknown function $f(t)$ satisfies a condition of the type

$$\int_0^{+\infty} \frac{f^2(t)}{P^2(t)}\,\mathrm{d}t < +\infty. \tag{1.10}$$

The requirement that $f(t)$ is exactly zero for $t < t_0$ and $t > t_1$ is replaced by the requirement that $f(t)$ is small outside a bounded region, provided that the 'profile' $P(t)$ is a smoothly varying function, tending to zero both when $t \to 0$ and $t \to \infty$.

Weighted L^2 spaces have already been used in inverse problems by Byrne and Fitzgerald [10] and by Byrne *et al* [11], but the singular bases and singular values were not computed and a special method of regularisation was employed. A full discussion of resolution limits and their relationship to a 'number of degrees of freedom' seems to require our present approach.

Assume that the average value of the particle radii is known (it can be essentially estimated from a preliminary analysis of the experimental data); then, if we introduce a scaling of the variables analogous to (1.5) (where now t_0 means the average value of the variable t) and a function $\chi(y)$ related to $\varphi(y)$ (defined as in equation (1.7)) by

$$\varphi(y) = P(y)\chi(y), \tag{1.11}$$

the problem is reduced to the inversion of the integral operator

$$(L\chi)(x) = \int_0^{\infty} K(xy)P(y)\chi(y)\,\mathrm{d}y. \tag{1.12}$$

Under suitable conditions on $P(y)$, the operator L is a compact operator from $L^2(0, +\infty)$ into $L^2(x_0, x_1)$ and the singular-value technique can also be used in this case.

In § 2 we give a short account of the main properties of the integral operator (1.9); some of the results are proved in two mathematical appendices. In § 3 we discuss the case of discrete data and, in particular, the cases of uniform sampling and geometric sampling of the data. In § 4 we give an outline of the inversion in weighted L^2 spaces and in § 5 we report some numerical results. We give examples of singular values and singular functions both in the case of bounded support and in the case of weighted reconstructions. Furthermore, the problem of resolution limits, discussed in I, is reconsidered in order to demonstrate the improvement due to localisation of the solution.

2. The case of continuous data and of a solution with bounded support

If we assume that the diffraction pattern is given everywhere on the range $[x_0, x_1]$, then the problem of determining the particle-radius distribution is equivalent to solving equation (1.8) or also to inverting the integral operator (1.9). As we have already remarked in the introduction, this integral operator is compact, since the integral kernel is bounded and continuous and the intervals where the functions are defined are bounded. Then we can introduce the singular system $\{\alpha_k; u_k, v_k\}_{k=0}^{+\infty}$ of the operator K, namely the set of the solutions of the coupled equations

$$Ku_k = \alpha_k v_k \qquad K^* v_k = \alpha_k u_k \tag{2.1}$$

where the adjoint operator K^* is given by

$$(K^*\psi)(y)=\int_{x_0}^{x_1} K(yx)\psi(x)\,dx \qquad 1\leqslant y\leqslant \gamma. \tag{2.2}$$

We assume, as usual, that the singular values are ordered to form a decreasing sequence: $\alpha_0\geqslant\alpha_1\geqslant\ldots$.

The singular functions u_k are also the eigenfunctions, associated with the eigenvalues α_k^2, of the self-adjoint, positive definite integral operator

$$(K^*K\varphi)(y)=\int_1^{\gamma} T(y,y')\varphi(y')\,dy' \qquad 1\leqslant y\leqslant \gamma \tag{2.3}$$

where

$$T(y,y')=\int_{x_0}^{x_1} K(yx)K(y'x)\,dx. \tag{2.4}$$

Analogously, the singular functions v_k are then eigenfunctions, also associated with the eigenvalues α_k^2, of the self-adjoint, positive definite integral operator

$$(KK^*\psi)(x)=\int_{x_0}^{x_1} S(x,x')\psi(x')\,dx' \qquad x_0\leqslant x\leqslant x_1 \tag{2.5}$$

where

$$S(x,x')=\int_1^{\gamma} K(xy)K(x'y)\,dy. \tag{2.6}$$

A first result is the following: both the operator K and the operator K^* are injective (invertible). We give the proof in the case of the operator K, since the case of the operator K^* is completely similar.

Indeed, assume that $K\varphi=0$; then the function $(K\varphi)(x)$, defined by equations (1.9) and (1.2), is zero over the interval $[x_0, x_1]$. Thanks to the analyticity of $J_1(x)/x$, the function $(K\varphi)(x)$ is also analytic and therefore it is zero everywhere. Using the eigenfunction expansions introduced in I, or alternatively the Mellin transform, we obtain

$$\tilde{K}(\tfrac{1}{2}+i\omega)\tilde{\varphi}(\tfrac{1}{2}-i\omega)=0 \tag{2.7}$$

where $\tilde{K}(\frac{1}{2}+i\omega)$ and $\tilde{\varphi}(\frac{1}{2}+i\omega)$ are the Mellin transforms of $K(x)$ and $\varphi(y)$ respectively. Since $\tilde{K}(\frac{1}{2}+i\omega)\neq 0$ for any ω (see I), it follows that $\tilde{\varphi}(\frac{1}{2}-i\omega)=0$ for any ω and therefore $\varphi(y)=0$.

The previous result implies that $\{u_k\}$ is a basis in $L^2(1,\gamma)$, while $\{v_k\}$ is a basis in $L^2(x_0,x_1)$. As a consequence, in the absence of noise, the solution of equation (1.11) is given by

$$\varphi(y)=\sum_{k=0}^{+\infty}\frac{1}{\alpha_k}(\psi,v_k)u_k(y) \tag{2.8}$$

where

$$(\psi,v_k)=\int_{x_0}^{x_1}\psi(x)v_k(x)\,dx. \tag{2.9}$$

In the presence of noise we will use the most simple regularisation technique, which is to truncate the series expansion (2.8).

We give now a few results describing the dependence of the singular values α_k on the parameter γ (characterising the support of the solution) and on the range of observation angles. To this purpose, let us denote by J the interval $[x_0, x_1]$ and by $\alpha_k(\gamma, J)$ the singular values of the operator (1.9). Then the following result is proved in appendix 1: *if* $\gamma \leqslant \gamma'$ *and also* $J \subset J'$, *then*

$$\alpha_k(\gamma, J) \leqslant \alpha_k(\gamma', J'). \tag{2.10}$$

In other words, for fixed k, the singular values of the problem are increasing functions both of the support of the solution and of the support of the data.

Furthermore, in appendix 2 it is proved that *when* γ *is large and the data support* J *tends to cover the half-line* $(0, +\infty)$, *the singular values* $\alpha_k(\gamma, J)$ *are given approximately by*

$$\alpha_k(\gamma, J) \sim 2^{-5/2} \left| \frac{\Gamma(\frac{5}{2} - i\omega_k)\Gamma(\frac{1}{4} + \frac{1}{2}i\omega_k)}{\Gamma^2(\frac{1}{4} - \frac{1}{2}i\omega_k)\Gamma(\frac{11}{4} - \frac{1}{2}i\omega_k)} \right| \tag{2.11}$$

where

$$\omega_k = \frac{\pi k}{\ln \gamma}. \tag{2.12}$$

Furthermore, for $k = 0$ *we have*

$$\alpha_0(\gamma, J) \leqslant \lambda_0^+ \tag{2.13}$$

where $\lambda_0^+ = 0.6271$ *is the largest 'eigenvalue' of the problem considered in I.*

The previous results give a qualitative description of the singular values as functions of the parameters characterising the problem. When both γ and the data support J are not large, only a numerical computation of the singular values is possible. They can be computed as the square roots of the eigenvalues of the integral operator (2.3) or, equivalently, of the integral operator (2.5). Numerical techniques for the computation of the eigenvalues and eigenfunctions of an integral operator, for example, as described in our previous publications, can be used. In the present case computations are more time consuming than in the other problems we have considered since the kernel (2.4) does not have a simple analytical form and therefore it can only be computed by means of quadrature formulae. However, in practice only the case with discrete data is interesting (see the next section) and therefore we have performed numerical computations only in this case.

We conclude this section by giving some approximate *symmetry properties* of the singular functions $u_k(y)$. If the range where the data are given is sufficiently large, so that in equation (2.4) we can extend the integral from 0 to $+\infty$ without introducing a large numerical error, then the operator K^*K, equations (2.3) and (2.4), takes the form

$$(K^*K\varphi)(y) = \int_1^\gamma H(y/y')\varphi(y')\,dy'/y' \tag{2.14}$$

where

$$H(y) = \int_0^{+\infty} K(y\xi)K(\xi)\,d\xi, \tag{2.15}$$

i.e. K^*K is a 'truncated' convolution operator. Then, by means of an elementary change of

variables, it is easy to show that, if $u(x)$ is an eigenfunction of K^*K associated with the eigenvalue α^2, the function

$$u_-(y)=\frac{\sqrt{\gamma}}{y}u\left(\frac{\gamma}{y}\right) \tag{2.16}$$

is also an eigenfunction of K^*K associated with the same eigenvalue α^2. Furthermore, if $u(y)$ is normalised to one with respect to the norm of $L^2(1, \gamma)$, then $u_-(y)$ is also normalised to one with respect to the same norm.

From the previous remark, it follows that, if an eigenvalue α_k^2 of K^*K has multiplicity one, then the corresponding eigenfunction $u_k(y)$ can only be *even*,

$$u_k(y)=\frac{\sqrt{\gamma}}{y}u_k\left(\frac{\gamma}{y}\right), \tag{2.17}$$

or *odd*,

$$u_k(y)=-\frac{\sqrt{\gamma}}{y}u_k\left(\frac{\gamma}{y}\right). \tag{2.18}$$

In particular the following relation is obtained for the boundary values of the singular functions:

$$|u_k(1)|=\sqrt{\gamma}|u_k(\gamma)|; \tag{2.19}$$

furthermore, in the case of odd eigenfunctions

$$u_k(\sqrt{\gamma})=0. \tag{2.20}$$

As shown by our numerical results (§ 5), in some cases these relations are rather well satisfied in spite of their approximate nature. An important feature is that, if we order the eigenvalues α_k^2 in a decreasing sequence, the corresponding singular functions are alternatively even and odd.

3. The case of discrete data and of a solution with bounded support

Assume now that the data function $\psi(x)$ is given only on a finite set of points $\xi_1, \xi_2, \ldots, \xi_N$, so that equation (1.11) is replaced by

$$\psi(\xi_n)=\int_1^\gamma K(\xi_n y)\varphi(y)\,\mathrm{d}y \qquad n=1,\ldots,N. \tag{3.1}$$

We denote by K_N the operator, defined by equation (3.1), which transforms a square-integrable function φ into an N-dimensional vector $\{\psi(\xi_n)\}_{n=1}^N$, which we call a data vector. Furthermore we assume that the space of data vectors is equipped with a scalar product having the form

$$(\psi_1, \psi_2)=\sum_{n=1}^N w_n\psi_1(\xi_n)\psi_2(\xi_n). \tag{3.2}$$

The introduction of the weights w_n, which will be specified in the following, can be justified by looking at (3.2) as an approximation of the usual product in the space of square-integrable functions.

Now, as follows from the definition of the scalar product (3.2), the adjoint operator K_N^*, which transforms a data vector into a function, is given by

$$(K_N^*\psi)(y)=\sum_{n=1}^{N} w_n K(y\xi_n)\psi(\xi_n). \tag{3.3}$$

The singular system $\{\alpha_{N,k};\, u_{N,k},\, v_{N,k}\}_{k=0}^{N-1}$ of the operator K_N is the set of the solutions of the coupled equations

$$K_N u_{N,k}=\alpha_{N,k} v_{n,k} \qquad K_N^* v_{N,k}=\alpha_{N,k} u_{N,k} \tag{3.4}$$

where $k=0,\ 1,\ \ldots,\ N-1$. Since the functions $K(y\xi_n)$ $(n=1,\ \ldots, N)$ are linearly independent, the operator K_N^* is injective and therefore the operator K_N has exactly N positive singular values $\alpha_{N,k}$. These are also the square roots of the eigenvalues of the finite-rank integral operator

$$(K_N^* K_N\varphi)(y)=\int_1^\gamma T_N(y, y')\varphi(y')\,\mathrm{d}y' \tag{3.5}$$

where

$$T_N(y, y')=\sum_{n=1}^{N} w_n K(y\xi_n)K(y'\xi_n) \tag{3.6}$$

or, equivalently, the square roots of the eigenvalues of the $N\times N$ matrix

$$(K_N K_N^*\psi)(x_n)=\sum_{m=1}^{N} S_{nm}^{(N)}\psi(\xi_m) \tag{3.7}$$

where

$$S_{nm}^{(N)}=w_m\int_1^\gamma K(\xi_n y)K(\xi_m y)\,\mathrm{d}y. \tag{3.8}$$

We notice that the kernel (3.6) appears as an approximation, given by some quadrature formula, of the kernel (2.4).

In this paper, as in our previous work on Laplace transform inversion [3, 4], we consider two data-point distributions: the first is a set of *equidistant points*

$$\xi_n=x_0+d(n-1) \qquad n=1,\ \ldots,\ N \tag{3.9}$$

where d, the distance between adjacent points, is such that $\xi_N=x_0+d(N-1)=x_1$ (x_0 and x_1 are the integration limits in equation (2.4)); the second is a set of points forming a *geometric progression*

$$\xi_n=x_0\Delta^{n-1} \qquad n=1,\ \ldots,\ N \tag{3.10}$$

where Δ, the ratio between adjacent points (dilation factor), is such that $\xi_N=x_0\exp[-\Delta(N-1)]=x_1$.

In the case of equidistant points we take constant weights,

$$w_n=d, \tag{3.11}$$

while in the case of points forming a geometric progression we take weights suggested by the sampling theorem [4],

$$w_n=(\ln\Delta)\xi_n. \tag{3.12}$$

For the choice (3.9) and (3.11) it is easy to prove that $T_N(y, y')$, equation (3.6), converges, uniformly over the square $[1, \gamma] \times [1, \gamma]$, to $T(y, y')$, equation (2.4), when $N \to \infty$ (or, equivalently, $d \to 0$). Analogously, for the choice (3.10) and (3.12), it is also possible to prove, by means of a suitable change of variable in the integral (2.4), that $T_N(y, y')$ converges uniformly to $T(y, y')$ when $N \to \infty$ (or, equivalently, $\Delta \to 1$). From this result one can prove, as in [4], that the singular values and singular functions, in the solution space, of the problem with discrete data converge to the singular values and singular functions of the problem with continuous data.

From the results we have obtained in the case of the Laplace transform inversion, it may be hoped that with only a moderate number of data points it should be possible to get satisfactory approximations of the singular values and singular functions of the problem with continuous data.

4. Inversion in weighted spaces

As we have outlined in the introduction, the solution of the integral equation (1.1) in a weighted L^2 space can be reduced to the inversion of the integral operator (1.12). When the data are given everywhere on the interval $[x_0, x_1]$, equation (1.12) defines an operator from $L^2(0, +\infty)$ into $L^2(x_0, x_1)$. Then the adjoint operator is given by

$$(L^*v)(y) = P(y) \int_{x_0}^{x_1} K(yx) v(x)\, dx \tag{4.1}$$

and therefore the operator L^*L has a kernel given by

$$T(y, y') = P(y)P(y') \int_{x_0}^{x_1} K(yx)K(y'x)\, dx. \tag{4.2}$$

The operator L^*L is of the trace class, and therefore the operator L is compact, when

$$\begin{aligned} \mathrm{Tr}(L^*L) &= \int_0^{+\infty} T(y, y)\, dy \\ &= \int_0^{+\infty} P^2(y) \left(\int_{x_0}^{x_1} K^2(yx)\, dx \right) dy < +\infty. \end{aligned} \tag{4.3}$$

Since $K(yx)$ is bounded and the integration interval $[x_0, x_1]$ is also bounded, condition (4.3) is satisfied provided that $P(y)$ is square integrable. An interesting example is provided by the gamma distribution

$$P(y) = \frac{\beta^\beta}{\Gamma(\beta)} y^{\beta-1} \exp(-\beta y) \qquad (\beta > 1) \tag{4.4}$$

whose mean value is one and whose variance is $1/\beta$. This particular profile function has been found very convenient in the case of Laplace transform inversion [9].

Denote by $\{\alpha_k; \varphi_k, v_k\}_{k=0}^{+\infty}$ the singular system of the operator L, where the φ_k are the eigenfunctions of the operator L^*L and the v_k are the eigenfunctions of the operator LL^*. Since both operators are injective, the φ_k form a basis in $L^2(0, +\infty)$ and the v_k form also a basis in $L^2(x_0, x_1)$. Therefore, by expanding the unknown function $\chi(y)$ as a series of the φ_k and recalling the relation (1.11), we find for $\varphi(y)$ a representation similar to (2.8) where

now the functions $u_k(y)$ are given by

$$u_k(y) = P(y)\varphi_k(y). \tag{4.5}$$

It is important to notice that the functions $\varphi_k(y)$ contain also a factor $P(y)$, as follows from the equation

$$\begin{aligned}\varphi_k(y) &= \alpha_k^{-1}(L^* v_k)(y) \\ &= \alpha_k^{-1} P(y) \int_{x_0}^{x_1} K(yx) v_k(x)\, dx.\end{aligned} \tag{4.6}$$

In particular it follows that $u_0(y)$ is roughly proportional to $P^2(y)$ since it is the product of $P^2(y)$ and of a positive slowly decreasing function.

The previous remarks imply that, if we consider a regularised solution of the problem, obtained by truncating the series expansion (2.8), this solution contains also $P^2(y)$ as a factor and therefore it is small precisely in those regions where the profile function is small.

The case of discrete data can be treated along the same lines as in § 3 by introducing an operator L_N transferring a function $\chi(y)$ of $L^2(0, +\infty)$ into an N-component data vector. Since the extension of the treatment given in § 3 is obvious, we omit the details.

5. Numerical results

We have performed some computations only in the case of discrete data using methods already described in [2–4].

In the case of an unknown function with bounded support and equidistant data points (§ 3) we have considered two values of γ ($\gamma = 5$ and $\gamma = 10$) and also two values of the cut-off in the diffraction pattern, corresponding respectively to the first and to the second zero of $J_1(x)/x$ ($x_1 = 3.832$ and $x_1 = 7.016$). We have used 24 points in the case of the smaller value of the cut-off and 48 in the other case. In both cases we have taken $x_0 = d$—see equation (3.9)—and therefore the two values of d are 0.160 and 0.146. We have computed the singular values greater than 10^{-3} and the results are reported in table 1. The results given in § 3 concerning the behaviour of the singular values as functions of γ and of

Table 1. Singular values for the problem with equidistant data points. In the case of 24 points the distance between adjacent points is $d = 0.160$; in the case of 48 points, $d = 0.146$.

	$\gamma = 5$		$\gamma = 10$	
α_k	$N = 24$	$N = 48$	$N = 24$	$N = 48$
α_0	0.3039	0.3065	0.3318	0.3364
α_1	0.9225×10^{-1}	0.9291×10^{-1}	0.1262	0.1286
α_2	0.3183×10^{-1}	0.3201×10^{-1}	0.5322×10^{-1}	0.5431×10^{-1}
α_3	0.1287×10^{-1}	0.1293×10^{-1}	0.2500×10^{-1}	0.2554×10^{-1}
α_4	0.6007×10^{-2}	0.6042×10^{-2}	0.1299×10^{-1}	0.1330×10^{-1}
α_5	0.3135×10^{-2}	0.3183×10^{-2}	0.7357×10^{-2}	0.7563×10^{-2}
α_6	0.1763×10^{-2}	0.1840×10^{-2}	0.4461×10^{-2}	0.4620×10^{-2}
α_7	0.1045×10^{-2}	0.1142×10^{-2}	0.2848×10^{-2}	0.2974×10^{-2}
α_8	—	—	0.1890×10^{-2}	0.1984×10^{-2}
α_9	—	—	0.1291×10^{-2}	0.1355×10^{-2}

the cut-off x_1 are confirmed by these computations also in the case of discrete data. The singular values are increasing functions of both γ and x_1.

In figure 1 we compare the singular-value spectra for $\gamma=5$ and $\gamma=10$, derived from table 1, with the eigenvalue spectrum calculated in I. The singular values are plotted associating to α_k a frequency ω_k given by equation (2.12) (ω_k is related to the resolution ratio, δ, by equation (5.1) below). It may be seen that, for practical values of the signal-to-noise ratio, say 10^2–10^3, the singular-value spectra lie above the eigenvalue spectrum. In other words, in spite of the fact that in the present case data are sampled and truncated, *a priori* knowledge of the support of the particle-size distributions improves the resolution limits computed in I slightly. However, at higher values of the signal-to-noise ratio, the singular-value spectrum lies below the eigenvalue spectrum. This follows as a consequence of the bounded support of the data, since then the singular values α_k fall off exponentially, as follows from general results of the behaviour of the eigenvalues of analytic kernels [12], while the eigenvalue spectrum computed in I tends to zero as ω^{-3}. At low signal-to-noise ratio the singular-value spectrum also falls below the eigenvalue spectrum as follows from the results proved in appendices 1 and 2.

For the intermediate region the improvement in resolution due to the knowledge of the support of the unknown function can be estimated as in [2] by defining a *resolution ratio* through the formula

$$\delta=\gamma^{1/K}=\exp(\pi/\omega_K) \tag{5.1}$$

where K is the index of the last term in the truncated singular-function expansion and ω_K

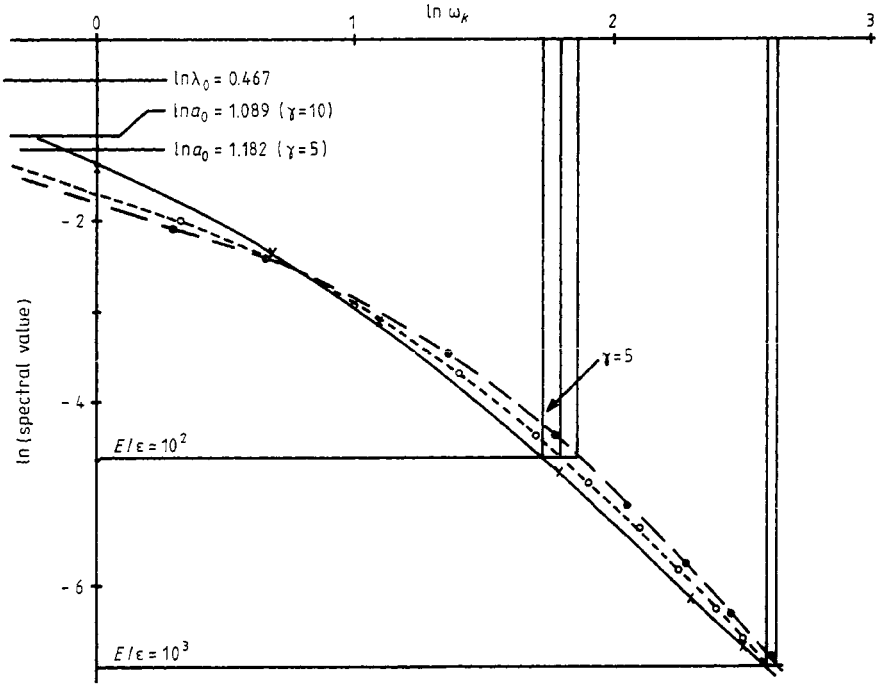

Figure 1. Comparison of the eigenvalue spectrum computed in I (full curve) with the singular-value spectrum in the case $\gamma=10$ (short broken curve) and in the case $\gamma=5$ (long broken curve) with 48 equidistant data points.

Table 2. Resolution ratio δ for various values of γ and of the signal-to-noise ratio E/ε.

E/ε	$\delta(\gamma=5)$	$\delta(\gamma=10)$	$\delta(\gamma=\infty)$
10^2	1.60	1.66	1.72
10^3	1.26	1.27	1.27

is defined in equation (2.12). For a given signal-to-noise ratio E/ε (defined as in [2]), K is the number of singular values satisfying the condition $\alpha_K \geqslant E/\varepsilon$. In the case $\gamma=\infty$, the resolution ratio δ was computed in I using truncated (generalised) eigenfunction expansions. We point out that in that paper the resolution was an upper bound since an unlimited support of the data was assumed.

In table 2 we compare some of the results obtained in I with the results which can be derived from table 1 and equation (5.1). As we see, the improvement in resolution due to *a priori* knowledge of the support seems to compensate the loss in resolution due to the finite support of the data, so that the results derived in I are quite good.

In figure 2 we give the singular functions corresponding to $\gamma=5$, $x_1=7.016$. As we see, the property (2.20) is satisfied approximately, indicating an approximate validity of the symmetry properties discussed in § 2. We notice that the values of the singular functions at the edges of the support $[1, \gamma]$ are rather large. This effect was already found by the authors in the case of Laplace transform inversion [4]; in fact, there is a surprising similarity of the singular functions of the two problems. As remarked in the introduction, this behaviour produces troublesome edge effects in the truncated singular-function expansion of the solution and it is the main motivation for the introduction of inversion methods in weighted spaces.

In the case $\gamma=5$ we have also investigated geometric sampling. More precisely, we have tried to reproduce the first eight singular values using only eight data points. Our results are very preliminary since, to save computations, we have fixed the cut-off x_1 at the value 3.832, corresponding to the first zero of $J_1(x)/x$, and we have considered only a few values of Δ. In table 3 we report some of the results we have obtained. The singular values in the geometric case are always smaller than the singular values in the linear case. However, it is interesting to remark that, in the case $\Delta=1.4$, the condition number α_0/α_7 is equal to 421 while in the case of linear sampling, with the same cut-off and 24 points, it is equal to 291. Therefore it is reasonable to argue that better results can be obtained if we change both Δ and x_1.

Table 3. Singular values in the case $\gamma=5$, using eight points forming a geometric progression for two values of the dilation factor Δ. In both cases the cut-off is $x_1=3.832$.

k	$\Delta=1.4$	$\Delta=1.6$
0	0.2248	0.2924
1	0.6652×10^{-1}	0.8962×10^{-1}
2	0.2476×10^{-1}	0.3086×10^{-1}
3	0.1066×10^{-1}	0.1231×10^{-1}
4	0.5441×10^{-2}	0.7630×10^{-2}
5	0.3565×10^{-2}	0.1395×10^{-2}
6	0.6862×10^{-3}	0.6646×10^{-3}
7	0.5334×10^{-3}	0.3662×10^{-3}

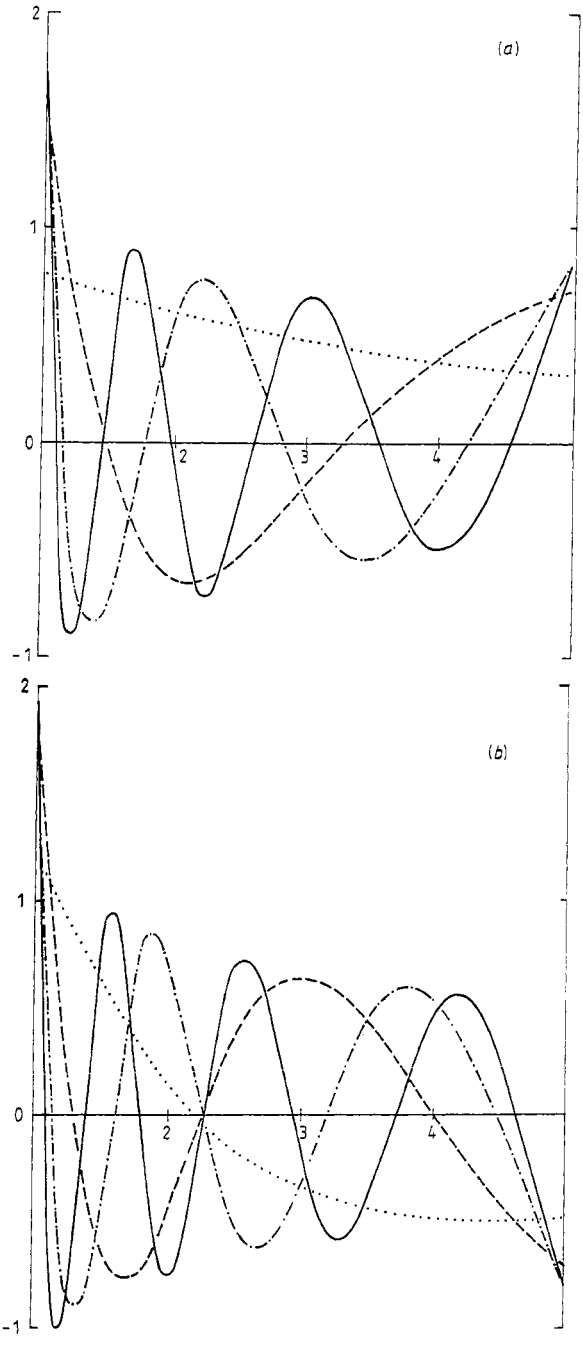

Figure 2. Singular functions in the case of an unknown function with bounded support and of 48 equidistant data points. Here $\gamma = 5$, $x_0 = 0.146$ and $x_1 = 7.016$—see equation (1.6). (*a*) Singular functions with k even: u_0 (dotted curve), u_2 (broken curve), u_4 (chain curve) and u_6 (full curve). (*b*) Singular functions with k odd: u_1 (dotted curve), u_3 (broken curve), u_5 (chain curve) and u_7 (full curve).

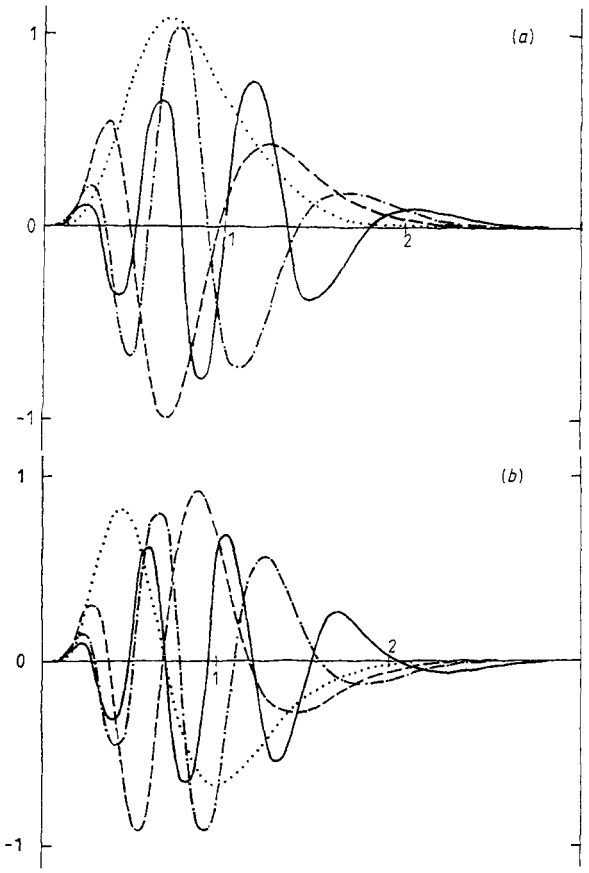

Figure 3. Singular functions in the case of a profile function of the type (4.4) with $\beta = 4$. Here $x_0 = 0.146$, $x_1 = 7.016$ and 48 linearly spaced points were used. (*a*) Singular functions with k even: u_0 (dotted curve), u_2 (broken curve); u_4 (chain curve) and u_6 (full curve). (*b*) Singular functions with k odd: u_1 (dotted curve), u_3 (broken curve), u_5 (chain curve) and u_7 (full curve).

Finally, we have considered the case of inversion in a weighted space. We have assumed a profile function of the type (4.4) with $\beta = 4$ and we have computed the singular values and singular functions in the case of 48 equidistant data points with a cut-off $x_1 = 7.016$. The first eight singular values are

$$\alpha_0 = 0.2360 \qquad \alpha_1 = 0.6073 \times 10^{-1} \qquad \alpha_2 = 0.2354 \times 10^{-1}$$
$$\alpha_3 = 0.1040 \times 10^{-1} \qquad \alpha_4 = 0.4742 \times 10^{-2} \qquad \alpha_5 = 0.2167 \times 10^{-2}$$
$$\alpha_6 = 0.9885 \times 10^{-3} \qquad \alpha_7 = 0.4487 \times 10^{-3}.$$

The ratio α_0/α_7 is equal to 526. The corresponding singular functions are given in figure 3. Subject to this condition number, therefore, any experimental particle-size distribution which may be made up using these components can be reconstructed by this method.

Acknowledgment

This work was partially supported by NATO grant no 463/84.

Appendix 1

In this appendix we prove the result contained in equation (2.10). First we prove that, for fixed J, $\alpha_k(\gamma, J)$ is an increasing function of γ and then we prove that, for fixed γ, $\alpha_k(\gamma, J)$ is an increasing function of J. By combining the two results, equation (2.10) follows.

In order to prove that $\alpha_k(\gamma, J)$ is an increasing function of γ for fixed J, recall that the eigenvalues of the operator (2.5) are just given by $\alpha_k^2(\gamma, J)$. Then, if $\gamma' > \gamma$, we have

$$\begin{aligned} S_{\gamma'}(x, x') &= \int_1^{\gamma'} K(xy)K(x'y)\,dy \\ &= \int_1^{\gamma} K(xy)K(x'y)\,dy + \int_{\gamma}^{\gamma'} K(xy)K(x'y)\,dy \\ &= S_{\gamma}(x, x') + R_{\gamma\gamma'}(x, x'). \end{aligned} \tag{A.1}$$

The integral operator whose kernel is $R_{\gamma\gamma'}(x, x')$ is positive definite since, for any ψ, we have

$$\int_{x_0}^{x_1} \psi(x)\left(\int_{x_0}^{x_1} R_{\gamma\gamma'}(x, x')\psi(x')\,dx'\right)dx = \int_{\gamma}^{\gamma'} \left(\int_{x_0}^{x_1} K(yx)\psi(x)\,dx\right)^2 dy \geqslant 0. \tag{A.2}$$

Therefore, by the Weyl–Courant lemma [12], assuming as usual that the eigenvalues of both the operator $(KK^*)_{\gamma}$ and the operator $(KK^*)_{\gamma'}$ are ordered to form decreasing sequences, the following inequality follows between eigenvalues corresponding to the same value of the index:

$$\alpha_k^2(\gamma, J) \leqslant \alpha_k^2(\gamma', J). \tag{A.3}$$

Take now γ fixed and assume that $J' \subset J$, namely $x_0' \leqslant x_0 < x_1 \leqslant x_1'$. In this case we use the fact that the $\alpha_k^2(\gamma, J)$ are the eigenvalues of the integral operator (2.3). Then, from equation (2.4) we get

$$\begin{aligned} T_{J'}(y, y') &= \int_{x_0'}^{x_1'} K(yx)K(y'x)\,dx \\ &= \int_{x_0}^{x_1} K(yx)K(y'x)\,dx + \int_{x_0'}^{x_0} K(yx)K(y'x)\,dx + \int_{x_1}^{x_1'} K(yx)K(y'x)\,dx \\ &= T_J(y, y') + R_{JJ'}(y, y'). \end{aligned} \tag{A.4}$$

Again, the integral operator whose kernel is $R_{JJ'}(y, y')$ is positive definite since we have

$$\begin{aligned} &\int_1^{\gamma} \varphi(y)\left(\int_1^{\gamma} R_{JJ'}(y, y')\varphi(y')\,dy'\right)dy \\ &\quad = \int_{x_0'}^{x_0} \left(\int_1^{\gamma} K(xy)\varphi(y)\,dy\right)^2 dx + \int_{x_1}^{x_1'} \left(\int_1^{\gamma} K(xy)\varphi(y)\,dy\right)^2 dx \geqslant 0 \end{aligned} \tag{A.5}$$

and, from the Weyl–Courant lemma it follows that

$$\alpha_k^2(\gamma, J) \leqslant \alpha_k^2(\gamma, J'). \tag{A.6}$$

Finally, by combining the inequalities (A.3) and (A.6), we get

$$\alpha_k^2(\gamma, J) \leqslant \alpha_k^2(\gamma, J') \leqslant \alpha_k^2(\gamma', J') \tag{A.7}$$

and equation (2.10) is proved.

Appendix 2

We prove here the asymptotic behaviour (2.11) and the inequality (2.13).

First we remark that, if $J_0 = [0, +\infty)$, then the arguments of the previous appendix can be applied to the case $J' = J_0$ and therefore, if we denote by $\alpha_k(\gamma)$ the singular values of the integral operator corresponding to J_0, we have

$$\alpha_k(\gamma, J) \leqslant \alpha_k(\gamma). \tag{A.8}$$

Furthermore, if we notice that the kernel

$$R_{JJ_0}(y, y') = \int_0^{x_0} K(yx)K(y'x)\,dx + \int_{x_1}^{+\infty} K(yx)K(y'x)\,dx \tag{A.9}$$

tends to zero uniformly with respect to $y, y' \in [1, \gamma]$ when $x_0 \to 0$ and also $x_1 \to +\infty$, from the Weyl–Courant lemma we derive also that

$$\lim_{x_0 \to 0,\, x_1 \to +\infty} \alpha_k(\gamma, J) = \alpha_k(\gamma). \tag{A.10}$$

In other words, the singular values $\alpha_k(\gamma, J)$, for fixed γ, tend from below to the singular values $\alpha_k(\gamma)$ when J tends to cover the half-line $[0, +\infty]$. Obviously this case is unphysical, but it gives upper bounds on the singular values of the physical case; furthermore the asymptotic behaviour of the singular values $\alpha_k(\gamma)$, when $\gamma \to +\infty$, can be easily derived.

Assume now that $J = J_0$ and denote by K_0 the corresponding integral operator. Then $K_0^* K_0$ is given by equations (2.14) and (2.15).

Now the Mellin transform of the function $H(y)$ is given by

$$H(\tfrac{1}{2} + i\omega) = \int_0^{+\infty} H(y)\, y^{-\frac{1}{2} + i\omega}\,dy = \tilde{K}(\tfrac{1}{2} + i\omega)\tilde{K}(\tfrac{1}{2} - i\omega) = |\tilde{K}(\tfrac{1}{2} + i\omega)|^2 \tag{A.11}$$

where, as shown in I, $\tilde{K}(\frac{1}{2} + i\omega)$, the Mellin transform of the function (1.2), is

$$\tilde{K}(\tfrac{1}{2} + i\omega) = \frac{2^{-\frac{1}{2} + i\omega}\,\Gamma(\frac{5}{2} - i\omega)\,\Gamma(\frac{1}{4} + \frac{1}{2}i\omega)}{\Gamma^2(\frac{7}{4} - \frac{1}{2}i\omega)\,\Gamma(\frac{11}{4} - \frac{1}{2}i\omega)}. \tag{A.12}$$

At this point, it is easy to prove as in [2] that, when $\gamma \to +\infty$,

$$\alpha_k^2(\gamma) \sim \tilde{H}(\tfrac{1}{2} + i\omega_k) = |\tilde{K}(\tfrac{1}{2} + i\omega_k)|^2 \tag{A.13}$$

where $\omega_k = \pi k / \ln \gamma$, $k = 0, 1, 2, \ldots$. Equation (2.11) follows from equations (A.10), (A.13) and (A.12).

Finally, in order to prove the inequality (2.10), we recall that α_0^2 is the supremum of the quadratic form associated with $K_0^* K_0$,

$$\alpha_0^2 = \sup \int_1^{\gamma} \varphi(y) \left(\int_1^{\gamma} T(y, y')\varphi(y')\,dy' \right) dy \tag{A.14}$$

over the boundary of the unit sphere, namely the set of the functions satisfying the condition

$$\int_1^{\gamma} \varphi^2(y)\,dy = 1. \tag{A.15}$$

Now, if we look at $L^2(1, \gamma)$ as a subspace of $L^2(0, +\infty)$, we have

$$\alpha_0^2 \leqslant \sup \int_0^{+\infty} \varphi(y) \left(\int_0^{+\infty} T(y, y')\varphi(y')\,dy' \right) dy \tag{A.16}$$

provided that

$$\int_0^{+\infty} \varphi^2(y)\,dy = 1. \tag{A.17}$$

Using the expression (2.4) for $T(y, y')$ we have

$$\begin{aligned} \alpha_0^2 &\leqslant \sup \int_{x_0}^{x_1} \left(\int_0^{+\infty} K(xy)\varphi(y)\,dy \right)^2 dx \\ &\leqslant \sup \int_0^{+\infty} \left(\int_0^{+\infty} K(xy)\varphi(y)\,dy \right)^2 dx = (\lambda_0^+)^2 \end{aligned} \tag{A.18}$$

where λ_0^+ is the supremum of the spectrum (maximum generalised eigenvalue) of the integral operator investigated in I. Since $\lambda_0^+ = |\tilde{K}(\frac{1}{2})|$, from (A.16) we have

$$\lambda_0^+ = 2^{-5/2} \frac{\Gamma(\frac{5}{2})\Gamma(\frac{1}{4})}{\Gamma^2(\frac{7}{4})\Gamma(\frac{11}{4})} = 0.6271 \tag{A.19}$$

and equation (2.13) is proved.

References

[1] Bertero M and Pike E R 1983 *Opt. Acta* **30** 1043–9
[2] Bertero M, Boccacci P and Pike E R 1982 *Proc. R. Soc.* A **383** 15–29
[3] Bertero M, Boccacci P and Pike E R 1984 *Proc. R. Soc.* A **393** 51–65
[4] Bertero M, Brianzi P and Pike E R 1984 *Proc. R. Soc.* A **398** 23–44
[5] Bertero M and Pike E R 1982 *Opt. Acta* **29** 727–46
[6] Bertero M, Boccacci P and Pike E R 1982 *Opt. Acta* **29** 1599–611
[7] Bertero M, Brianzi P, Parker P and Pike E R 1984 *Opt. Acta* **31** 181–201
[8] Bertero M, De Mol C, Pike E R and Walker J G 1984 *Opt. Acta* **31** 923–46
[9] Bertero M, Brianzi P and Pike E R 1985 *Inverse Problems* **1** 1–15
[10] Byrne C L and Fitzgerald R M 1982 *SIAM J. Appl. Math.* **42** 933
[11] Byrne C L, Fitzgerald R M, Fiddy M A, Hall T J and Darling A M 1983 *J. Opt. Soc. Am.* **73** 1481
[12] Hille E and Tamarkin T D 1931 *Acta Math.* **57** 1–76